Phase Field Theory of Heterogeneous Crystal Nucleation

László Gránásy,[1] Tamás Pusztai,[1] David Saylor,[2] and James A. Warren[3]
[1]*Research Institute for Solid State Physics and Optics, H-1525 Budapest, P.O.B. 49, Hungary*
[2]*Food and Drug Administration, Rockville, Maryland 20852, USA*
[3]*National Institute of Standards and Technology, Gaithersburg, Maryland 20899, USA*
(Received 15 June 2006; published 18 January 2007)

The phase field approach is used to model heterogeneous crystal nucleation in an undercooled pure liquid in contact with a foreign wall. We discuss various choices for the boundary condition at the wall and determine the properties of critical nuclei, including their free energy of formation and the contact angle as a function of undercooling. For particular choices of boundary conditions, we may realize either an analog of the classical spherical cap model or decidedly nonclassical behavior, where the contact angle decreases from its value taken at the melting point towards complete wetting at a critical undercooling, an analogue of the surface spinodal of liquid-wall interfaces.

DOI: 10.1103/PhysRevLett.98.035703 PACS numbers: 64.60.Qb, 64.70.Dv, 82.60.Nh

Heterogeneous nucleation is not only a phenomenon of classic importance in materials science, but also remains one of continuously growing interest, due to the emerging technological interest in nanopatterning techniques and control of related nanoscale processes [1]. While solidification of pure undercooled liquids is initiated by homogeneous nucleation (the formation of small crystalline fluctuations exceeding a critical size determined by the interplay of the driving force of crystallization and the interfacial free energy [2]), the presence of foreign particles, container walls, and other heterogeneities typically facilitates this process [3]. Despite its vast technological importance, heterogeneous nucleation remains poorly understood. This deficit stems from the complexity of describing the interaction between the foreign matter and the solidifying melt.

Wetting of a foreign wall by fluids or crystals has been studied extensively [4] including such phenomena as critical wetting and phase transitions at interfaces [5]. Various methods have been applied to address these problems such as continuum models [6] and atomistic simulations [7]. Despite this inventory, recent studies [8] addressing heterogeneous crystal nucleation rely almost exclusively on the classical spherical cap model, which assumes mathematically sharp interfaces [9]. Here the wall-liquid and wall-solid interactions are characterized by the contact angle θ that is determined from the interfacial free energies by Young's equation: $\gamma_{WL} = \gamma_{WS} + \gamma_{SL}\cos(\theta)$, where subscripts W, S, and L refer to the wall, the solid, and the liquid, respectively. Such models qualitatively describe this system, but lose their applicability [2] when the size of nuclei is comparable to the interface thickness (the nanometer range, according to atomistic simulations [2,10]). Such nanoscale nuclei are essentially "all interface." Recent investigations show [11] that phase field theory (PFT, [12]) can address this issue. Indeed, PFT can quantitatively predict the nucleation barrier for systems (e.g, hard-sphere, Lennard-Jones, ice-water) where the necessary input data are available. We therefore adopt this approach to describe heterogeneous nucleation. Experimentally, the details of the wall-fluid interaction are embedded in more directly accessible quantities, such as the contact angle in equilibrium. It is thus desirable to develop a model that describes the wall in such phenomenological terms. Along this line, interaction between dendritic growth and wall has recently been discussed in [13], while Castro addressed crystal nucleation in a specific case of $\theta = 90°$, obtained by prescribing "no-flux" boundary condition at the wall [14]. A more general treatment is, however, required.

In this Letter, we describe how to implement phase field methods of heterogeneous nucleation with an arbitrary contact angle. For simplicity, we consider a single component system, whose local state is characterized by the nonconserved phase field $\phi(\mathbf{r})$, monitoring the structural transition ($\phi = 0$: crystal; $\phi = 1$: liquid). Following previous work [5,6], we assume that the interaction of the wall with the solidifying system is of sufficiently short range to be characterized by a "contact free energy" $\gamma_W(\phi)$ that depends only on the local state of matter abutting the wall. Then the free energy of the system consists of a surface and a volumetric contribution

$$F_{\mathrm{tot}} = \int_A dA\gamma_W(\phi) + \int_V dV\left[\frac{\epsilon^2 T}{2}(\nabla\phi)^2 + f(\phi)\right]. \quad (1)$$

Here A is a closed surface bounding volume V of the solid-liquid system. At A, the system is in contact with the wall. The local free energy density, given the temperature T, is assumed to be $f(\phi) = wTg(\phi) + [1 - p(\phi)]f_S(T) + p(\phi)f_L(T)$, while the "double well" and "interpolation" functions have the forms $g(\phi) = (1/4)\phi^2(1-\phi)^2$ and $p(\phi) = \phi^3(10 - 15\phi + 6\phi^2)$ [12]. The model parameters can be related to the solid-liquid interface free energy, the interface thickness δ, and the melting temperature T_m as $\epsilon^2 = 2^{1/2}6\gamma_{SL}\delta/T_m$ and $w = 2^{1/2}6\gamma_{SL}/(T_m\delta)$.

 © 2007 The American Physical Society

The critical fluctuation (nucleus) represents an extremum of the free energy. The extremum condition $\delta F_{\mathrm{tot}} = 0$ yields the following equations:

$$\frac{\partial \gamma_W}{\partial \phi} - \epsilon^2 T(\mathbf{n} \cdot \nabla \phi) = 0 \quad \text{on } A; \tag{2}$$

$$\frac{\partial f}{\partial \phi} - \epsilon^2 T(\nabla^2 \phi) = 0. \tag{3}$$

Here $\mathbf{n}$ is the normal vector pointing away from the wall, and Eq. (2) is the boundary condition on A to Eq. (3), which in turn is the differential Euler-Lagrange (EL) equation to be satisfied inside the volume V.

We consider first a semi-infinite system in contact with a wall. We label the phase field at the wall ϕ_0, and in the far field ϕ_∞. The free energy has three possible extrema in this case: (i) stable solid in contact with the wall ($\phi_\infty = 0$; absolute minimum); (ii) metastable liquid in contact with the wall ($\phi_\infty = 1$; local minimum); (iii) unstable solid droplet (critical fluctuation) formed in metastable liquid at the wall ($\phi_\infty = 1$; saddle point).

To advance further, we must specify the contact free energy $\gamma_W(\phi)$ or require ϕ_0 be constant. In general, either of these conditions will be fixed by the details of the wall-fluid interaction. Thus, we now consider two illustrative choices for our boundary conditions and relate these choices to the equilibrium contact angle.

Model A.—We assume that the wall does not perturb the structure of the planar solid-liquid interface. Then $|\nabla\phi|$ can be calculated using the one dimensional version of the integral of Eq. (3) (at $T = T_m$): $(\epsilon^2 T/2)(\nabla\phi)^2 = f(\phi) - f(\phi_\infty) = \Delta f(\phi)$, and the normal component of the gradient at the wall can be expressed as $\mathbf{n} \cdot \nabla\phi = |\nabla\phi| \cos(\theta)$. Combining these expressions, we have

$$\mathbf{n} \cdot \nabla \phi = [\cos(\theta)/(2^{1/2}\delta)]\phi_0(1 - \phi_0); \quad \text{on } A, \tag{4}$$

a condition that coincides with [14] for $\theta = 90°$. The respective contact free energy, obtained by integrating Eq. (2), reads as $\gamma_W(\phi) - \gamma_{WL} = -\gamma_{SL}\cos(\theta) \times [2\phi^3 - 3\phi^2 + 1]$. Given the postulated relationship between $\cos(\theta)$ and the interfacial free energies, we find $\gamma(\phi) = \gamma_{WS} - \gamma_{WL}$ at the wall-solid contact and $\gamma(\phi) = 0$ at the wall-liquid contact. We adopt Eq. (4) and the respective $\gamma_W(\phi)$ in the undercooled state. Model A can thus be viewed as a phase field implementation of the classical spherical cap model similar in spirit to that by Semoroz *et al.* [13].

Model B.—Alternatively, we may specify $\phi_0 = \text{const.}$, a mathematical analog of the condition used for describing liquid spreading on a wall in [15], but where the order parameter is now not the density, but instead applies to the nonconserved crystallinity order parameter appropriate to a liquid-solid system. Thus, the physical meaning of the boundary condition (liquid ordering) differs significantly from the one in [15]. For planar interfaces at the melting point, the interfacial free energies can be expressed as $\gamma_{WL} = h(\phi_0, 1) + \gamma_0$, $\gamma_{WS} = h(0, \phi_0) + \gamma_0$, and $\gamma_{SL} = h(0, 1)$, where

$$h(\phi_1, \phi_2) = \int_{\phi_1}^{\phi_2} d\phi [2\epsilon^2 T \Delta f(\phi)]^{1/2}. \tag{5}$$

After some algebra, we find $\cos(\theta) = (\gamma_{WL} - \gamma_{WS})/\gamma_{LS} = 1 - 6\phi_0^2 + 4\phi_0^3$. The condition that $\phi_0 = \text{const.}$ sets the degree of ordering (in the case of liquid next to the wall) or disordering (in the case of solid abutting the wall). Inspection of the integral EL equation indicates a behavior akin to surface spinodal known for liquid-wall interfaces [5]. A metastable liquid solution exists for $\Delta f(\phi_0) > 0$, i.e., below a critical undercooling ΔT_s given by the condition $\Delta f(\phi_0) = 0$. (As ϕ_0 approaches the solid state, ΔT_s converges to 0.) At lower T, there is no time-independent solution of this type; instead, a propagating solidification front emerges that is described by the usual equation of motion for the phase field [16].

Our choices of the boundary condition correspond to two distinct physical situations: (a) the ''classical'' case, when liquid ordering is negligible at the wall, and (b) a ''nonclassical'' case, where there is ordering at the wall. This structure is of a specific nature, as it corresponds to the particular, chosen level of ordering as one traverses solid-liquid interface. As such, this order is ''compatible'' with the appearing crystal and will lower the nucleation barrier to the formation of solid. While it is typical for liquids to order at an abutting wall [7(c),10(b),10(d)], such ordering may not be compatible with the structure to which the liquid crystallizes [4], and a more detailed model would be required. Based on these observations, we expect that our combined analyses of Models A and B will elucidate many of the essential behaviors of physical systems. In what follows, we evaluate the properties of heterogeneous nuclei in these two limiting cases, and present illustrative simulations for pure Ni [17].

The EL equation for the composite system nucleus plus undercooled liquid has been solved by the finite element method. The initial condition has been created by placing the classical sharp interface nucleus into the simulation window after broadening its interface by a tanh function of appropriate width parameter. The simulation box had the size of 30 nm × 20 nm. The equation of motion for dynamic evolution simulations was solved in a dimensionless form using the finite difference method and parallel computing on a PC cluster of 120 nodes. The spatial step was $\Delta x = 0.2$ nm, while noise (as described in [14]), has been added to the governing equation.

Critical fluctuations (nuclei) computed at undercooling $\Delta T = 35$ K as a function of the equilibrium contact angle θ are presented in Fig. 1. For comparison, Fig. 2 shows the nuclei calculated for a contact angle of $\theta = 61.2°$ ($\phi_0 = 1/3$) as a function of ΔT. While in both models the size of heterogeneous nuclei becomes comparable to the interface thickness with increasing undercooling, in Model B, it happens at a far smaller undercooling. It is remarkable that while the contact angle is approximately constant in Model A, in Model B, it varies drastically with under-

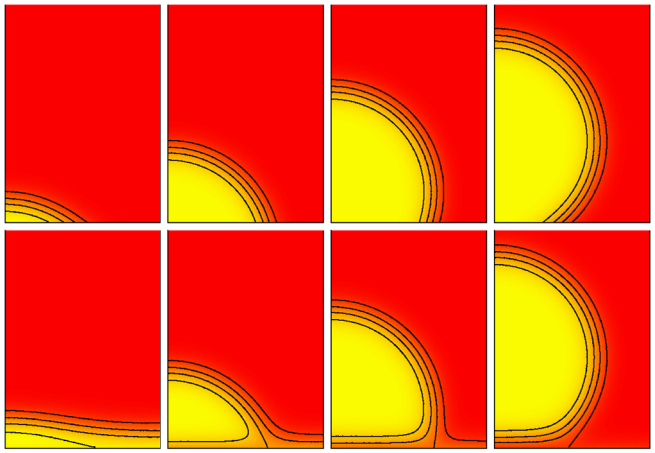

FIG. 1 (color online). Structure of heterogeneous nuclei in 2D vs equilibrium contact angle at $\Delta T = 35$ K in Model A (upper row) and B (lower row). From left to right $\theta = 37.6°$, 72.8°, 107.2°, and 142.3° ($\phi_0 = 0.2$, 0.4, 0.6, and 0.8). The contour lines stand for $\phi = 0.2$, 0.4, 0.6, and 0.8. Horizontal size is 10 nm. For symmetry reasons, only the right half of the nuclei is shown.

cooling in Model B, and tends to 0° complete wetting at the critical undercooling. The free energy of heterogeneous nuclei in Model A and B are also shown in Fig. 2. For Model A, it has been calculated by integrating the free energy density difference relative to the bulk undercooling liquid and adding the contribution from the wall. For Model B, the integrated free energy of the wall-liquid system has been subtracted from the free energy of the wall-nucleus-liquid system. It is found that the free energies of nuclei from Models A and B fall close to the values from the sharp interface spherical cap model (2D) for small undercoolings where the nuclei are large relative to the interface thickness, while lower values are obtained at larger undercoolings. In Model B, the nucleation barrier disappears at ΔT_s. Atomistic simulations could test the existence of such a surface spinodal for freezing.

Next, we demonstrate that our approach allows for modeling of an important practical case: the micromechanism of inoculation of undercooled liquids by foreign particles whose different surfaces are characterized by different contact angles [18]. The classical model for cylindrical particles predicts that to establish free growth of the crystal, the udercooling needs to exceed a critical value $\Delta T_c = 4\gamma_{SL} T_m (Ld)^{-1}$, where d is the diameter of the cylindrical particle, and L is the volumetric heat of fusion. For $\Delta T < \Delta T_c$, a stable hemispherical crystal is expected. Our simulations are in full agreement with the classical picture if noise is switched off after nucleation. However, a significant reduction of ΔT_c is predicted once the physical noise is used throughout the simulation (Fig. 3). These results suggest that the capillary waves induced by thermal noise destabilize the hemispherical stable state. For $\Delta T > \Delta T_c$, a transient period is observed to precede free growth.

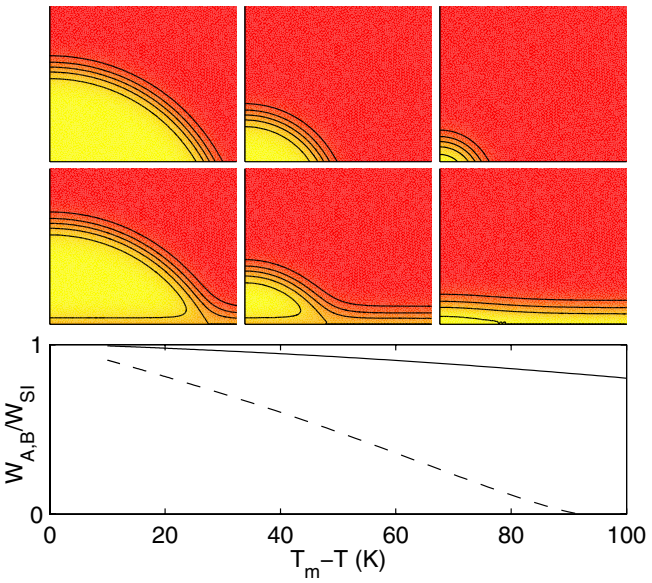

FIG. 2 (color online). Structure of nuclei in 2D at three undercoolings ($\Delta T = 20$ K, 40 K, and 90 K) in Models A (upper row) and B (central row), at an equilibrium contact angle of $\theta = 61.2°$, corresponding to $\phi_0 = 1/3$ and $\Delta T_c = 92.0$ K. The contour lines indicate $\phi = 1/6$, 2/6, 3/6, 4/6, and 5/6, respectively. Horizontal size is 12 nm. The free energy of nonclassical nuclei ($W_{A,B}$) normalized by the sharp interface prediction (W_{SI}) is also shown as a function of undercooling (bottom panel): Model A—solid line; Model B—dashed line.

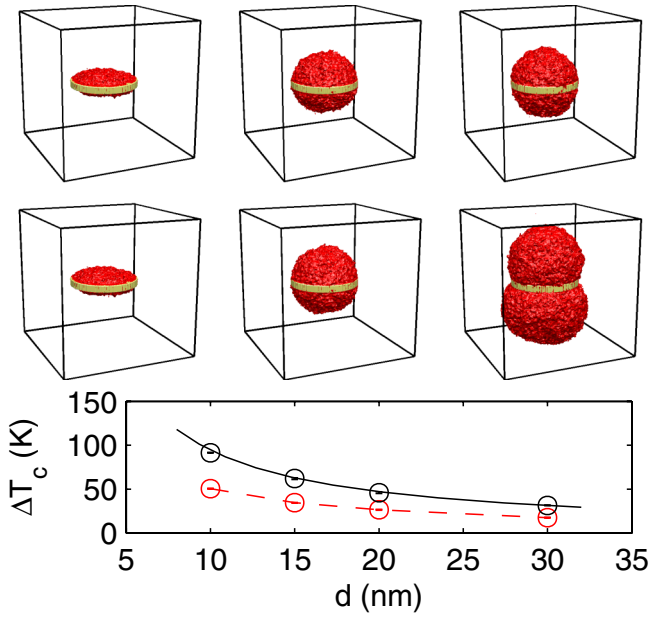

FIG. 3 (color online). Micromechanism of inoculation of undercooled Ni by cylindrical particles ($d = 20$ nm) with contact angles of 45° and 175° on the horizontal and vertical surfaces, respectively, as predicted by Model A. [200 × 200 × 200 grid.] Upper row: $\Delta T = 26$ K $< \Delta T_c$, $t = 25$, 250, 1000 ns; central row: $\Delta T = 27$ K $> \Delta T_c$, $t = 25$, 250, 750 ns; bottom row: ΔT_c vs particle diameter d. Classical—solid line; simulation—dashed line.

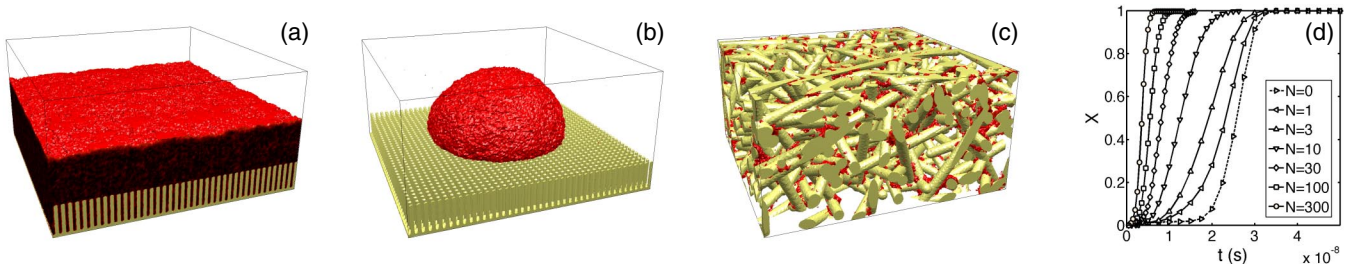

FIG. 4 (color online). Phase field simulation of nucleation on patterned and random nanofiber networks in 3D using Model A. On nanofiber ''brush'' composed of vertically aligned nanofibers with (a) uniform ($\theta = 75°$), and (b) different contact angles for the horizontal (75°) and vertical sides (175°). Note, the drastically different crystallization patterns for (a) and (b) due to different wetting on the vertical sides of the ''brush.'' (c) Nucleation on a random nanofiber network ($\theta = 75°$). (d) Increasing amount of nanofibers accelerates crystallization, as reported for carbon nanotube-polymer composites [1]. (X—crystalline fraction; t—time. $\Delta T = 175$ K. The simulation box is 100 nm × 100 nm × 50 nm.

These predictions should be verifiable by experiment or atomistic simulations.

Further illustrative simulations, demonstrating the power of our approach, are presented in Fig. 4 that shows nucleation on patterned and random nanofiber networks. Such simulations are expected to find applications in nanopatterning studies and in research on nanocomposites [1].

We have developed a phase field methodology to describe heterogeneous crystal nucleation in undercooled liquids at walls characterized by arbitrary contact angles. Two limiting cases have been addressed: (Model A) Nucleation at surfaces where liquid ordering at the wall is negligible and (Model B) where the wall-liquid interaction induces partial crystalline order in the liquid. Using the prescriptions described above, many other boundary conditions can be explored. Note that this approach can be directly extended to existing phase field models of alloy and anisotropic polycrystalline systems characterized by further fields. The present study thus opens up new ways for modeling heterogeneous nucleation in a broad variety of systems.

The authors acknowledge helpful discussions with J. W. Cahn and G. B. McFadden. This work has been supported by Contracts No. OTKA-K-62588, ESA PECS No. 98005, and by the EU FP6 Project IMPRESS under Contract No. NMP3-CT-2004-500635.

[1] J. Aizenberg, A. J. Black, and G. M. Whitesides, Nature (London) **398**, 495 (1999); J. D. Hartgelink, E. Beniash, and S. I. Stupp, Science **294**, 1684 (2001); B. P. Grady *et al.*, J. Phys. Chem. B **106**, 5852 (2002).

[2] S. Auer and D. Frenkel, Nature (London) **409**, 1020 (2001); D. Moroni, P. R. ten Wolde, and P. G. Bolhuis, Phys. Rev. Lett. **94**, 235703 (2005).

[3] S. Auer and D. Frenkel, Phys. Rev. Lett. **91**, 015703 (2003).

[4] For review see: D. Bonn and D. Ross, Rep. Prog. Phys. **64**, 1085 (2001); A. Esztermann and H. Löwen, J. Phys. Condens. Matter **17**, S429 (2005).

[5] J. W. Cahn, J. Chem. Phys. **66**, 3667 (1977); M. R. Moldover and J. W. Cahn, Science **207**, 1073 (1980).

[6] J. D. van der Waals, Verhand. Kon. Akad. v. Wetensch. (Ie Cest.) **1**, 1 (1893); E. M. Blokhuis, Phys. Rev. E **51**, 4642 (1995); B. Widom, J. Phys. Chem. **99**, 2803 (1995); V. Talanquer and D. W. Oxtoby, J. Chem. Phys. **104**, 1483 (1996).

[7] (a) K. Yasuoka, G. T. Gao, and X. C. Zeng, J. Chem. Phys. **112**, 4279 (2000); (b) A. Milchev, A. Milchev, and K. Binder, Comput. Phys. Commun. **146**, 38 (2002); (c) E. B. Webb, III, G. S. Grest, and D. R. Heine, Phys. Rev. Lett. **91**, 236102 (2003).

[8] For example: J. H. Perepezko, Mater. Sci. Eng. A **413**, 389 (2005); J. H. Perepezko and W. S. Tong, Philos. Mag. **361**, 447 (2004).

[9] R. D. Gretz, J. Chem. Phys. **45**, 3160 (1966).

[10] (a) For example: *Experiment:* W. J. Huisman *et al.*, Nature (London) **390**, 379 (1997); (b) J. M. Howe and H. Saka, MRS Bull. **29**, 951 (2004); (c) *Atomistic simulations:* B. B. Laird and A. D. J. Haymet, Chem. Rev. **92**, 1819 (1992); (d) P. Geysermans, D. Gorse, and V. Pontikis, J. Chem. Phys. **113**, 6382 (2000).

[11] L. Gránásy, J. Mol. Struct. **485–486**, 523 (1999); L. Gránásy and T. Pusztai, J. Chem. Phys. **117**, 10 121 (2002); L. Gránásy, T. Börzsönyi, and T. Pusztai, Phys. Rev. Lett. **88**, 206105 (2002).

[12] Recent reviews on the phase field method: J. J. Hoyt, M. Asta, and A. Karma, Mater. Sci. Eng. Rep. R **41**, 121 (2003); L. Gránásy, T. Pusztai, and J. A. Warren, J. Phys. Condens. Matter **16**, R1205 (2004).

[13] A. Semoroz, S. Henry, and M. Rappaz, Metall. Mater. Trans. A **31**, 487 (2000); B. P. Athreya *et al.*, Philos. Mag. **86**, 3739 (2006).

[14] M. Castro, Phys. Rev. B **67**, 035412 (2003).

[15] L. M. Pismen and Y. Pomeau, Phys. Rev. E **62**, 2480 (2000).

[16] S. L. Wang *et al.*, Physica D (Amsterdam) **69**, 189 (1993).

[17] Properties of pure Ni were used: $T_m = 1728$ K, heat of fusion $L = 2.666 \times 10^9$ J/m^3, $\gamma_{SL} = 0.364$ J/m^2, free energy difference $f_L - f_S = L(T_m - T)/T_m$. The 10%–90% interface thickness was assumed to be 2 nm.

[18] A. L. Greer *et al.*, Acta Mater. **48**, 2823 (2000).